

Controlling Orbital Moment and Spin Orientation in CoO Layers by Strain

S. I. Csiszar,¹ M. W. Haverkort,² Z. Hu,² A. Tanaka,³ H. H. Hsieh,⁴ H.-J. Lin,⁵ C. T. Chen,⁵ T. Hibma,¹ and L. H. Tjeng²

¹Materials Science Center, University of Groningen, Nijenborgh 4, 9747 AG Groningen, The Netherlands

²II. Physikalisches Institut, Universität zu Köln, Zùlpicher Strasse 77, 50937 Köln, Germany

³Department of Quantum Matter, ADSM, Hiroshima University, Higashi-Hiroshima 739-8530, Japan

⁴Chung Cheng Institute of Technology, National Defense University, Taoyuan 335, Taiwan

⁵National Synchrotron Radiation Research Center, 101 Hsin-Ann Road, Hsinchu 30077, Taiwan

(Received 8 November 2004; published 28 October 2005)

We have observed that CoO films grown on different substrates show dramatic differences in their magnetic properties. Using polarization dependent x-ray absorption spectroscopy at the Co $L_{2,3}$ edges, we revealed that the magnitude and orientation of the magnetic moments strongly depend on the strain in the films induced by the substrate. We presented a quantitative model to explain how strain together with the spin-orbit interaction determine the $3d$ orbital occupation, the magnetic anisotropy, as well as the spin and orbital contributions to the magnetic moments. Control over the sign and direction of the strain may, therefore, open new opportunities for applications in the field of exchange bias in multilayered magnetic films.

DOI: [10.1103/PhysRevLett.95.187205](https://doi.org/10.1103/PhysRevLett.95.187205)

PACS numbers: 75.25.+z, 71.70.-d, 75.70.-i, 78.70.Dm

The discovery of the exchange bias phenomenon in surface-oxidized cobalt particles about 50 years ago [1] marks the beginning of a new research field in magnetism. Since then, several combinations of antiferromagnetic (AFM) and ferromagnetic (FM) thin film materials have been fabricated and investigated [2,3], motivated by the potential for applications in information technology. Numerous theoretical [4–8] and experimental [9–14] studies have been devoted to unravel the mechanism(s) responsible for exchange biasing. However, no conclusive picture has emerged yet. A major part of the problem lies in the fact that there is insufficient information available concerning the atomic and magnetic structure of the crucial interface between the AFM and FM material. The important issue of, for instance, spin reorientations in the AFM films close to the interface is hardly considered [15–19], and the role of epitaxial strain herein has not been discussed at all.

In this paper, we study the magnetic properties of CoO thin films epitaxially grown on MnO(100) and on Ag(100), as model systems for an AFM material under either tensile or compressive in-plane stress. Our objective is to establish how the magnetic anisotropy as well as the spin and orbital contributions to the magnetic moments depend on the lowering of the local crystal field symmetry by epitaxial strain. Using polarization dependent x-ray absorption spectroscopy (XAS) at the Co $L_{2,3}$ ($2p \rightarrow 3d$) edges, we observe that the magnitude and orientation of the magnetic moments in the CoO/MnO(100) system are very different from those in CoO/Ag(100). We present a quantitative model to calculate how local crystal fields together with the spin-orbit interaction determine the magnetic properties.

The actual compositions of the CoO/MnO(100) and CoO/Ag(100) systems are (14 Å)MnO/(10 Å)CoO/(100 Å)MnO/Ag(001) and (90 Å)CoO/Ag(001), respec-

tively. The two samples were grown by molecular beam epitaxy (MBE), evaporating elemental Mn and Co from alumina crucibles in a pure oxygen atmosphere of 10^{-7} to 10^{-6} mbar. The base pressure of the MBE system is in the low 10^{-10} mbar range. The thickness and epitaxial quality of the films are monitored by reflection high energy electron diffraction measurements. With the lattice constant of bulk Ag (4.09 Å) being smaller than that of bulk CoO (4.26 Å) and MnO (4.444 Å), we find from x-ray diffraction that CoO on Ag is slightly compressed in-plane ($a_{\parallel} \approx 4.235$ Å, $a_{\perp} \approx 4.285$ Å) and from reflection high energy electron diffraction that CoO sandwiched by MnO is about 4% expanded in-plane ($a_{\parallel} \approx 4.424$ Å). The sandwich structure was used to maximize the CoO thickness with full in-plane strain. Details about the growth will be published elsewhere [20].

The XAS measurements were performed at the Dragon beam line of the National Synchrotron Radiation Research Center (NSRRC) in Taiwan using *in situ* MBE grown samples. The spectra were recorded using the total electron yield method in a chamber with a base pressure of 3×10^{-10} mbar. The photon energy resolution at the Co $L_{2,3}$ edges ($h\nu \approx 770$ – 800 eV) was set at 0.3 eV, and the degree of linear polarization was $\approx 98\%$. The sample was tilted with respect to the incoming beam, so that the Poynting vector of the light makes an angle of $\alpha = 70^\circ$ with respect to the [001] surface normal. To change the polarization, the sample was rotated around the Poynting vector axis as depicted in Fig. 1, and θ , the angle between the electric field vector \vec{E} and the [001] surface normal, can be varied between 20° and 90° . This measurement geometry allows for an optical path of the incoming beam which is independent of θ , guaranteeing a reliable comparison of the spectral line shapes as a function of θ . A CoO single crystal is measured *simultaneously* in a separate chamber to obtain

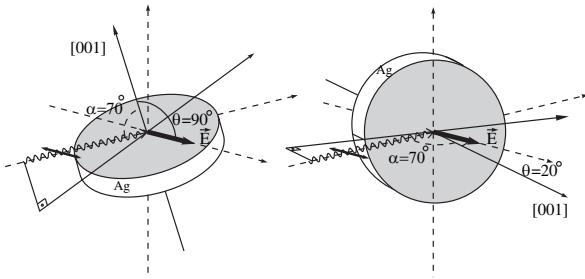


FIG. 1. Experimental XAS geometry, with polarization of the light in the horizontal plane. θ is the angle between the electric field vector \vec{E} and the [001] surface normal, and α is the tilt between the Poynting vector and the surface normal.

a relative energy reference with an accuracy of better than 0.02 eV.

Figure 2 shows the polarization dependent Co $L_{2,3}$ XAS spectra of the CoO/MnO(100) (left panels) and CoO/Ag(100) (right panels) systems, taken at temperatures both far below (top panels) and far above (bottom panels) the Néel temperature of the CoO thin film, which is about 290 K for CoO/MnO(100) and 310 K for CoO/Ag(100) as we will show below. The angle θ between the electric field vector \vec{E} and the [001] surface normal is varied between 20° and 90° . The spectra have been corrected for electron yield saturation effects [21]. The general line shape of the spectra shows the characteristic features similar to that of bulk CoO [22], ensuring the good quality of our CoO films. Very striking in the spectra is the clear polarization dependence, which is stronger at 77 K than at 400 K. Important also is that the polarization dependence of the CoO/MnO(100) system is opposite to that of the CoO/Ag(100): For instance, the intensity of the

first peak at $h\nu = 777$ eV is always higher for $\theta = 20^\circ$ than for $\theta = 90^\circ$ in CoO/MnO(100), while it is always smaller in CoO/Ag(100).

In order to resolve the origin of the polarization dependence in the CoO spectra, we have investigated the temperature dependence in more detail. Figure 3(a) depicts the polarization contrast of the peak at $h\nu = 777$ eV, defined as the difference divided by the sum of the peak height in the spectra taken with the $\theta = 20^\circ$ and $\theta = 90^\circ$ polarizations. One can clearly see a significant temperature dependence for both systems, and a closer look also reveals the presence of a kink at about 290 K for CoO/MnO(100) and 310 K for CoO/Ag(100), which can be associated with the Néel temperatures of the CoO thin films as we will show below. We therefore infer that at high temperatures the polarization contrast is caused solely by crystal field effects and that at low temperatures the magnetism must also contribute to the contrast. In other words, we are observing crystal field induced linear dichroism at high temperatures and a combination of crystal field induced and magnetic linear dichroism at low temperatures. Important is to note that the opposite sign in the dichroism for the CoO/MnO(100) and CoO/Ag(100) systems implies that the orientation of the magnetic moments is perpendicular and the sign of the crystal field splittings is opposite in the two systems.

To analyze the Co $L_{2,3}$ spectra quantitatively, we perform calculations for the atomiclike $2p^63d^7 \rightarrow 2p^53d^8$ transitions using a similar method as described by Alders *et al.* [23] but now in a D_{4h} point group symmetry and including covalency. The method uses a CoO₆ cluster which includes the full atomic multiplet theory and the local effects of the solid [22,24]. It accounts for the intra-atomic $3d$ - $3d$ and $2p$ - $3d$ Coulomb and exchange interac-

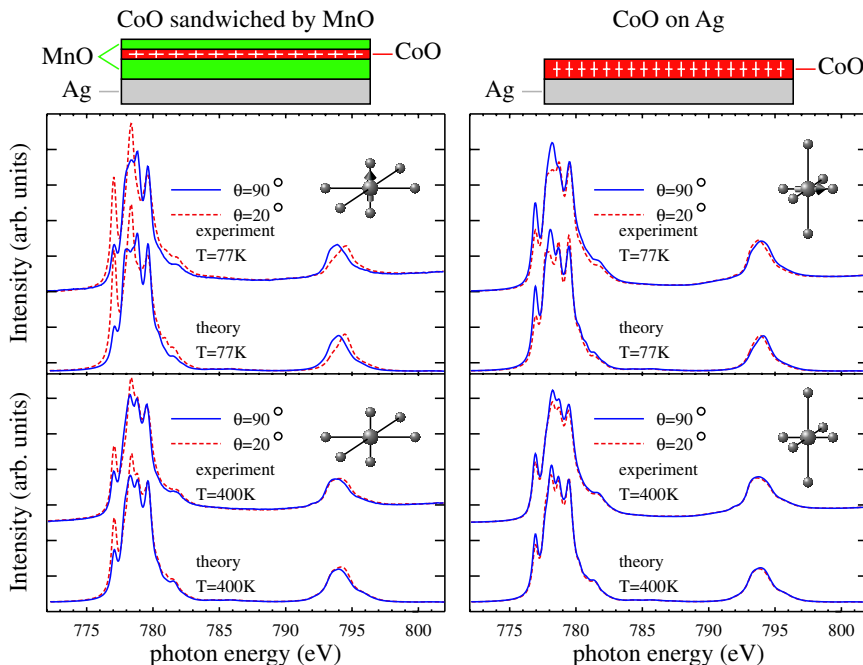


FIG. 2 (color online). Experimental and calculated Co $L_{2,3}$ XAS spectra of (left panel) CoO in (14 Å)MnO/(10 Å)CoO/(100 Å)MnO/Ag(001) at $\theta = 20^\circ$ and $\theta = 90^\circ$, far below (top panel, $T = 77$ K) and far above (bottom panel, $T = 400$ K) the Néel temperature of the CoO thin film; (right panel) the same for CoO in (90 Å)CoO/Ag(001).

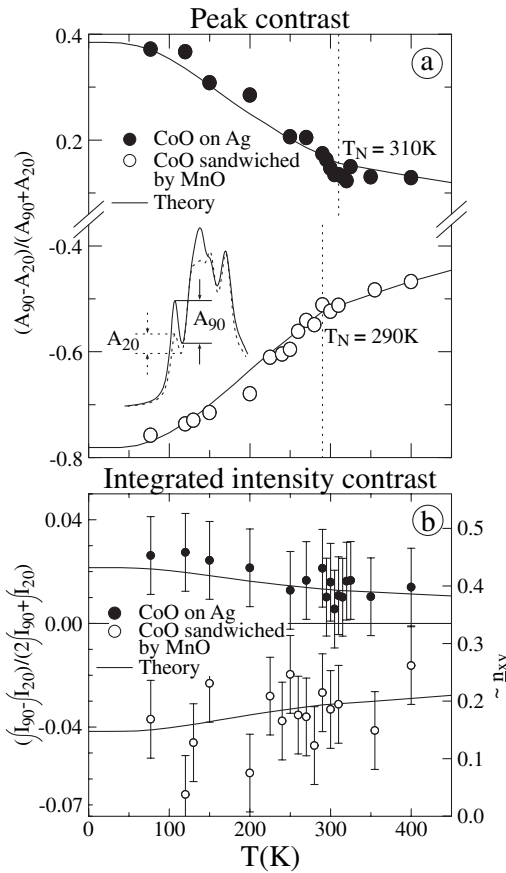


FIG. 3. Temperature dependence of the polarization contrast in the Co $L_{2,3}$ spectra: (a) peak contrast, defined as the difference divided by the sum of the height of the first peak at $h\nu = 777$ eV, taken with $\theta = 20^\circ$ and $\theta = 90^\circ$ polarizations; (b) integrated intensity contrast, defined as the difference divided by the sum of the intensity, integrated over the entire $L_{2,3}$ range. Solid and empty circles are the experimental data. The solid lines are the theoretical simulations.

tions, the atomic $2p$ and $3d$ spin-orbit couplings, the O $2p$ —Co $3d$ hybridization, local crystal field parameters $10Dq$, Ds , and Dt , and a Brillouin-type temperature dependent exchange field which acts on spins only and which vanishes at T_N . The calculations have been carried out using the XTLS 8.0 program [24].

The results of the calculations are shown in Fig. 2. We have used the parameters already known for bulk CoO [24,25] and have to tune only the parameters for Ds , Dt , and the direction of the exchange field. For the CoO/MnO(100) system, we find an excellent simulation of the experimental spectra for $Ds = -40$ meV, $Dt = -13$ meV, and an exchange field parallel to the $[001]$ surface normal. For the CoO/Ag(100) system, we obtained the best fit for $Ds = 13$ meV, $Dt = 4$ meV, and an exchange field perpendicular to the $[001]$ surface normal. These two sets of parameters reproduce extremely well the spectra at all temperatures, as is also demonstrated in Fig. 3(a), showing the excellent agreement between the

calculated and measured temperature dependent polarization contrast of the first peak. Most important is obviously the information that can be extracted from these simulations. We find that the magnetic moments in CoO/MnO(100) are oriented out of plane, and, in strong contrast, those in CoO/Ag(100) are in-plane. We also find for CoO/MnO(100) a $2.46\mu_B$ spin and $1.36\mu_B$ orbital contribution to the $3.82\mu_B$ total magnetic moment. By comparison, the numbers for CoO/Ag(100) are smaller: 2.14, 1.00, and $3.14\mu_B$, respectively. The crystal field parameters give also a very different splitting in the t_{2g} levels: about -56 meV for CoO/MnO(100) and $+18$ meV for CoO/Ag(100), which is fully consistent with our structural data in that the CoO in CoO/MnO(100) experiences a *large* in-plane *expansion* (tensile strain) while the CoO in CoO/Ag(100) is only *slightly contracted* in-plane (compressive strain).

Shape anisotropy cannot explain why the spin of the thinner CoO film, i.e., CoO/MnO(100), is oriented out of plane while that of the thicker film, i.e., CoO/Ag(100), is in-plane. In order to understand intuitively the important interplay between strain and spin-orbit interaction for the magnetic properties of materials with a partially filled $3d$ t_{2g} shell, we will start with describing the energetics of the high spin Co^{2+} ($3d^7$) ion in a one-electron-like picture. In O_h symmetry, the atomic $3d$ levels are split into 3 t_{2g} and 2 e_g orbitals, so that two holes reside in the spin-down e_g orbitals and one hole in one of the spin-down t_{2g} . Introducing a tetragonal distortion, in which the c axis (out of plane) is made different from the a axis (in-plane), the t_{2g} levels also become split. In the limit that this splitting is much larger than the spin-orbit interaction, we will find for CoO with $c/a \ll 1$ that the t_{2g} hole will occupy a linear combination of d_{xz} and d_{yz} orbitals. The spin-orbit interaction will then produce a $m_l = -1$ state, i.e., a state with an orbital moment of $1\mu_B$ directed perpendicular to the plane of the film. The spin moment will be also out of plane, since it is coupled via the spin-orbit interaction to the orbital moment. For CoO with $c/a \gg 1$, we will get a t_{2g} hole in the d_{xy} orbital, i.e., a state with a quenched orbital momentum [26]. For the actual CoO/Ag(100) system, we find that c/a is indeed larger than 1 but only slightly and with a t_{2g} splitting which is smaller than the spin-orbit interaction. As a result, the orbital moment is not quenched [27]. In fact, it is directed in-plane and, thus, also the spin moment. For the CoO/MnO(100) system, the c/a is smaller than 1, and the orbital and spin moment are indeed directed out of plane. The size of the orbital moment as calculated in the cluster model is somewhat larger than $1\mu_B$, but this is merely due to the presence of Coulomb and exchange interactions in the multiplet structure [27,28] not considered in the simple one-electron picture.

The fact that strain has a direct influence on the orbital occupation, as revealed by our theoretical analysis, can also be verified experimentally. In Fig. 3(b) we plot the

difference divided by the sum of the integrated Co $L_{2,3}$ intensities for the two polarizations for a wide range of temperatures. The integration is over the entire Co $L_{2,3}$ spectral region, and a background has been subtracted following the prescription often used in evaluating orbital moment sum rules in soft-x-ray magnetic circular dichroism spectroscopy [29]. One can clearly observe that there is a significant nonzero polarization contrast in the integrated intensities and that this contrast has an opposite sign for the two systems studied here. It is important to realize that the integrated intensity for a particular polarization of the light depends merely on the symmetry of the $3d$ holes in the initial state. To illustrate this, let us make the simplification that 2 holes reside in the spin-down e_g orbitals and 1 hole in one of the spin-down t_{2g} . We then have [27]

$$\frac{\int I_{90} - \int I_0}{2 \int I_{90} + \int I_0} = \frac{\underline{n}_{xy} - \frac{1}{2}(\underline{n}_{xz} + \underline{n}_{yz})}{2\underline{n}_{\text{total}}}, \quad (1)$$

where \underline{n} denotes the hole number and the subscript the orbital type. For an isotropic orbital occupation, the integrated contrast would be 0 and $\underline{n}_{xy} = 1/3$. One can now directly deduce from the data that the CoO/Ag(100) system has relatively more d_{xy} holes than the CoO/MnO(100), fully consistent with $c/a > 1$ in CoO/Ag(100) and $c/a < 1$ in CoO/MnO(100). The cluster calculations reproduce the measured integrated polarization contrast very well and reveal that the actual \underline{n}_{xy} [27] is about 0.4 and 0.2, respectively, for the two systems.

Based on the parameters extracted from the excellent simulations of the spectra, we have estimated the magnetocrystalline anisotropy within the CoO films. We calculated the single ion anisotropy by comparing the total energy of the CoO_6 cluster for different exchange field directions. This energy is expressed as $E = K_0 + K_1 \sin^2(\eta) + K_2 \sin^4(\eta) + K_3 \sin^4(\eta) \sin^2(\varphi) \cos^2(\varphi)$, where η is the angle between the exchange field and the c axis, and φ is the azimuthal angle. We find for CoO/MnO(100) $K_1 = 3.4$ meV, $K_2 = 1.4$ meV, and $K_3 = 0.1$ meV, while for CoO/Ag(100) we obtain $K_1 = -1.7$ meV, $K_2 = 0.1$ meV, and $K_3 = 0.1$ meV. In other words, for CoO/MnO(100) the energy difference between the spin directed parallel with the easy axis ($\eta = 0^\circ$, perpendicular to the film) and parallel with the hard axis ($\eta = 90^\circ$, lying in the film plane) is about 4.8 meV. The same single ion anisotropy energy calculated for the CoO/Ag(100) is about -1.6 meV, i.e., the hard axis is perpendicular and the easy axis parallel to the film plane. These energies are more than 2 orders of magnitude larger than the dipolar anisotropy within the film [30].

To conclude, CoO films grown on different substrates show dramatic differences in their magnetic properties. Strain induced local crystal fields together with the spin-orbit interaction determine the $3d$ orbital occupation, the magnetic anisotropy, as well as the spin and orbital contributions to the magnetic moments. Control over the sign

and direction of the strain may, therefore, open new opportunities for applications in the field of exchange bias in multilayered magnetic films, especially when using magnetic ions with a partially filled t_{2g} shell.

We acknowledge the NSRRC staff for providing us with an extremely stable beam. We thank Lucie Hamdan and Henk Bruinenberg for their skillful technical and organizational assistance in preparing the experiment. The research in Cologne is supported by the Deutsche Forschungsgemeinschaft through SFB 608.

-
- [1] W.H. Meiklejohn and C.P. Bean, Phys. Rev. **102**, 1413 (1956); **105**, 904 (1957).
 - [2] See, for review, J. Nogués and I.K. Schuller, J. Magn. Magn. Mater. **192**, 203 (1999).
 - [3] See, for review, A.F. Berkowitz and K. Takano, J. Magn. Magn. Mater. **200**, 552 (1999).
 - [4] A.P. Malozemoff, Phys. Rev. B **35**, R3679 (1987).
 - [5] D. Mauri *et al.*, J. Appl. Phys. **62**, 3047 (1987).
 - [6] N.C. Koon, Phys. Rev. Lett. **78**, 4865 (1997).
 - [7] T.C. Schulthess and W.H. Butler, Phys. Rev. Lett. **81**, 4516 (1998).
 - [8] M.D. Stiles and R.D. McMichael, Phys. Rev. B **59**, 3722 (1999).
 - [9] K. Takano, R.H. Kodama, A.E. Berkowitz, W. Cao, and G. Thomas, Phys. Rev. Lett. **79**, 1130 (1997).
 - [10] P.J. van der Zaag *et al.*, Phys. Rev. Lett. **84**, 6102 (2000).
 - [11] H. Ohldag *et al.*, Phys. Rev. Lett. **87**, 247201 (2001).
 - [12] H. Ohldag *et al.*, Phys. Rev. Lett. **91**, 017203 (2003).
 - [13] J. Camarero *et al.*, Phys. Rev. Lett. **91**, 027201 (2003).
 - [14] A. Scholl, M. Liberati, E. Arenholz, H. Ohldag, and J. Stohr, Phys. Rev. Lett. **92**, 247201 (2004).
 - [15] M.J. Carey, A.E. Berkowitz, J.A. Borchers, and R.W. Erwin, Phys. Rev. B **47**, 9952 (1993).
 - [16] Y. Ijiri *et al.*, Phys. Rev. Lett. **80**, 608 (1998).
 - [17] J.A. Borchers *et al.*, J. Appl. Phys. **83**, 7219 (1998).
 - [18] H. Ohldag *et al.*, Phys. Rev. Lett. **86**, 2878 (2001).
 - [19] F. Radu *et al.*, Phys. Rev. B **67**, 134409 (2003).
 - [20] S.I. Csiszar and T. Hibma (to be published).
 - [21] R. Nakajima, J. Stöhr, and Y.U. Idzerda, Phys. Rev. B **59**, 6421 (1999).
 - [22] See review by F.M.F. de Groot, J. Electron Spectrosc. Relat. Phenom. **67**, 529 (1994).
 - [23] D. Alders *et al.*, Phys. Rev. B **57**, 11 623 (1998).
 - [24] A. Tanaka and T. Jo, J. Phys. Soc. Jpn. **63**, 2788 (1994).
 - [25] Parameters for CoO_6 cluster: $\Delta = 6.5$, $U_{dd} = 6.5$, $U_{cd} = 8.2$, $pd\sigma = -1.2$, $T_{pp} = 0.7$, $10Dq = 0.525$, $\zeta = 0.066$, $H_{ex} = 0.0126$; Slater integrals 80% of Hartree Fock values; CoO/MnO(100): $D_s = -0.040$, $D_t = -0.013$; CoO/Ag(100): $D_s = 0.013$, $D_t = 0.004$; all values in eV.
 - [26] T. Jo and T. Shishidou, J. Phys. Soc. Jpn. **67**, 2505 (1998).
 - [27] M.W. Haverkort *et al.* (to be published).
 - [28] S. Sugano, Y. Tanabe, and H. Kamimura, *Multiplets of Transition-Metal Ions in Crystals* (Academic, New York, 1970).
 - [29] C.T. Chen *et al.*, Phys. Rev. Lett. **75**, 152 (1995).
 - [30] M. Finazzi and S. Altieri, Phys. Rev. B **68**, 054420 (2003).